

# A Novel Compact UHF Wideband Antenna for Near Field Electrical Characterization of Steel Fiber Reinforced Concrete

G. Roqueta<sup>#1</sup>, S. Irteza<sup>\*</sup>, J. Romeu<sup>#</sup> and L. Jofre<sup>#</sup>

<sup>#</sup>*Signal Theory and Communications Department, Universitat Politècnica de Catalunya  
Spain*

<sup>#1</sup>*gemma.roqueta@tsc.upc.edu*

<sup>\*</sup>*Royal Institute of Technology (KTH)  
Sweden*

**Abstract**— A novel, electrically small, UHF (350 MHz–750 MHz) microstrip slot antenna is presented. The antenna is designed for the characterization of Steel Fiber Reinforced Concrete (SFRC) segments. The antenna consists on a three layer structure headed by the slot ground plane, followed by the feeding microstrip in the central layer with some resistive loading for bandwidth enhancement purposes; finally on the bottom layer a strip line reflector is positioned to provide a unidirectional radiation pattern, required for harsh environments. The whole design has been optimized in front of SFRC for maximum impedance bandwidth. Input impedance and radiation pattern are studied both theoretically and experimentally, and some laboratory measurements have been done on real SFRC specimens. Satisfactory results for the fiber density of SFRC are presented.

## I. INTRODUCTION

Thanks to its excellent mechanical properties, Steel Fiber Reinforced Concrete (SFRC) is being increasingly used in civil constructions that need to withstand heavy forces such as pavements, airport runways and subway tunnels [1]. In this kind of materials, fibers are mixed with fresh concrete, providing more flexibility and less fabrication cost than the conventional hand-tied rebars, while still increasing the tensile strength many times. The mixing needs to be performed with extreme care, since uniform density and random orientation of fibers are crucial for uniform and isotropic strength properties of the segment. Nowadays, destructive methods are mainly used to assess dosage and uniformity of fiber distribution. Slabs are basically analysed pointwise, by drilling out a core, crushing and counting the number of fibers using magnets. Other less common methods can be found, based on acoustic [2], spectroscopic [3], or non-destructive local inspection. The latter being a local method does not provide the global information of a whole piece of concrete as it is desirable for civil engineering, while the formers present high interferences and low repeatability.

The lack of fast and precise non-destructive quality testing methods concerning both the method and the instrumentation, motivates the development of a novel compact wideband antenna which relies on the use of microwaves, as a promising method able to provide a fair trade off between resolution and penetrability, and to ensure the robustness of concrete in terms

of homogeneous fiber distribution. Wideband condition implies the use of a large band of the spectrum that offers a big range of advantages in the scope of embedded objects characterization. Mainly, resolution is highly improved with respect to the conventional narrowband systems where the reconstructed resonances are highly sensitive to the operating frequency band.

In this paper, a compact, electrically small and light weighted antenna solution is presented. This design considers the antenna as an integrated element to the medium in order to avoid losses and undesired reflections in near field measurements, so the natural medium for the antenna is the concrete itself. The presented wideband antenna design consists on a slot antenna [4][7] supported on a FR-4 substrate  $\epsilon_r=4.4$  of thickness  $h=1.6\text{mm}$  and  $19\times 22\text{cm}^2$  surface area, with a tuning fork microstrip coupled feeding [5]. This compact form provides a good trade off between wide impedance bandwidth and antenna size reduction. The tuning fork broadbanding technique compensates for the bandwidth reduction derived from the antenna size reduction due to minimization purposes. The use of resistive loading provides a smoothed time domain pulse contributing to higher impedance bandwidth. Finally a compact light weight strip line reflector is added to avoid background noise contributions during measurements in harsh environments such as civil engineering workshop.

Numerical analysis is performed with Ansoft High-frequency Structure Simulator (HFSS), which is based on finite element method. Measurements are conducted to verify this novel antenna performance by Agilent E8362B Network Analyser. Details of the proposed slot antenna are described. Simulated and measured results of impedance bandwidth and the radiation characteristics are given and discussed in this paper.

## II. ANTENNA DESIGN

Fig. 2 shows the prototype of the wideband cavity backed slot antenna presented in this paper. Fig. 2 and Fig. 3 show the three dimensional view and exploded view of the antenna.

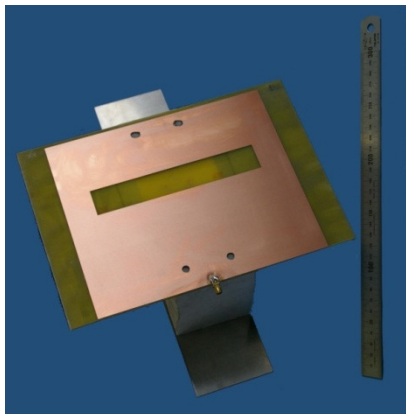


Fig. 1 Prototype of a wideband cavity backed slot antenna.

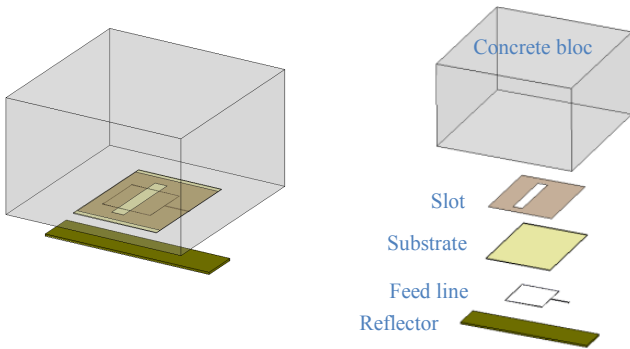


Fig. 2 Prototype of a wideband cavity backed slot antenna.

Fig. 3 Exploded view of the proposed antenna

Antenna design parameters are calculated keeping in consideration the requirement of operating frequency band from 350 MHz to 700 MHz at-least, as indicated in [6]. The design dimensions are shown in Fig. 4.

Slot resonant frequency is mainly dependent on the slot length which should be approximately half of an effective wavelength. In this design, slot length  $L_{slot}$  is taken to be  $\lambda_g/2$ , where  $\lambda_g$  is  $\frac{\lambda_0}{\sqrt{\epsilon_{rs}}}$  at 400 MHz.  $\epsilon_{rs}$  is calculated using the equation

$$\epsilon_{rs} = \frac{\epsilon_{rconc} + \epsilon_r}{2} \quad (1)$$

where  $\epsilon_{rconc} = 6$  is the effective relative permittivity of dry concrete reported in previous literatures, and  $\epsilon_r = 4.4$  is the effective relative permittivity of the FR-4 substrate.

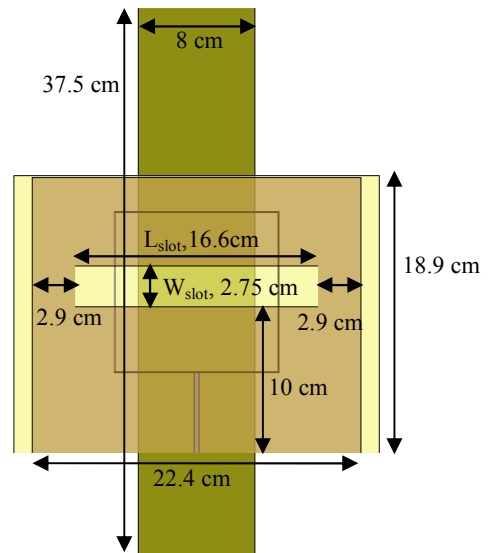


Fig. 4 Geometry and dimensions of the proposed antenna.

The self inductance of the slot is related to the slot width  $W_{slot}$ . Many authors have shown that increasing the width of the slot can result in a greater impedance bandwidth [8], so this parameter is optimized according to this criteria resulting  $W_{slot} = 0.16 \cdot L_{slot}$ . The ground plane is also optimized according to minimum dimension and reasonable bandwidth criteria. The final size of the ground plane is  $0.3\lambda_0 \times 0.25\lambda_0$ , being thereby considered a compact electrically small UHF antenna.

As it is shown in Fig. 2, a strip line reflector based on an evolution of a conventional cavity based back-lobe suppressor has been added below the feeding line, in order to be compliant with the uni-directionality requirement derived from the need to avoid background interferences. The reflector dimensions and separation distance play an important role in volumetric dimensions of the complete antenna, as well as in antenna behaviour in terms of radiation and bandwidth. The reflector cancels out the backward radiation and provides gain in endfire direction. However, this option reduces the impedance bandwidth. To compensate for this bandwidth reduction effect, the width of the reflector can be reduced while still maintaining reasonable bandwidth and front to back ratio. Hence, the reduction of the reflector distance combined with the reduction of reflector width, contributes to a global reduction of the antenna size and weight, while still preserving its radiation and good bandwidth properties. Reflector dimensions (8cm  $\times$  37.5cm) and separation (10cm) are adjusted to achieve maximum impedance bandwidth and a front-to-back ratio greater than 10dB at the working frequency band. Fig. 7 shows the effect of the reflector distance concerning return losses. The closer the reflector is to the ground plane, the narrower is the bandwidth.

### III. FEED LINE

A microstrip dual offset feeding line is used as a broadbanding technique in this design. Feed line structure consists of a 50Ω impedance line divided into dual offset 100Ω lines. The dimensions of the feed line are shown in Fig. 5. In order to achieve the specified characteristic impedance in FR-4 substrate, the width of the transmission line  $W_t$  is calculated using [7]

$$z_{ct} = \frac{60}{\sqrt{\epsilon_{rt}}} \ln \left[ \frac{8h}{W_t} + \frac{W_t}{4h} \right] \quad \frac{W_t}{h} \leq 1 \quad (2a)$$

$$z_{ct} = \sqrt{\epsilon_{rt}} \left[ \frac{W_t}{h} + 1.393 + 0.667 \ln \left( \frac{W_t}{h} + 1.444 \right) \right] \quad \frac{W_t}{h} \geq 1 \quad (2b)$$

Where  $z_{ct}$  is the characteristic impedance of the line,  $h$  is the height of the substrate and  $\epsilon_{rt}$  is the relative permittivity of the substrate.

The length of the feeding fork arms  $L_{fork}$  is calculated as  $L_{fork} = \frac{\lambda_0}{4\sqrt{\epsilon_{rt}}}$  according to [9]. The offset distance between the two feeding lines has to be adjusted in order to obtain maximal impedance bandwidth, and so it is chosen to be  $D_f = \frac{\lambda_g}{4}$  where  $\lambda_g$  is the waveguide wavelength of the slot.

In order to remove the possible ringing effects in the transmitted signal, a loading technique is employed in this design. A 1.1kΩ resistor is appended on the open circuit connection of the feeding fork. This also provides a wide impedance matching since the reactive component of the antenna is absorbed by the use of these resistors. Although radiation efficiency is slightly reduced to 60 %, near-field measurements are not really concerned by this effect since the received power is high enough to achieve a reasonable level of signal to noise ratio (SNR).

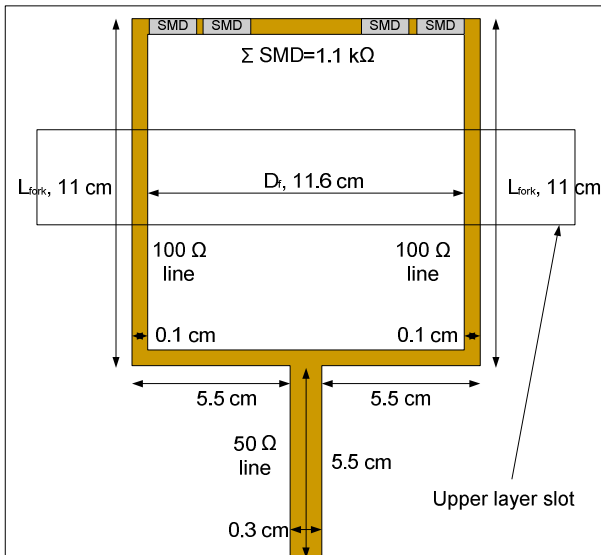


Fig. 5 Geometry and dimensions of the feed line.

### IV. ANTENNA PERFORMANCE RESULTS

The measured and simulated return loss parameter of the proposed antenna is shown in Fig. 6. In simulations with standard dry concrete, a 75 % fractional bandwidth (FRB) is achieved, which is compliant with the initial requirements of the antenna. In measurements, FRB depends on the type of concrete to be analysed, but it is estimated that it can oscillate between 75% and 90% in the best of the cases.

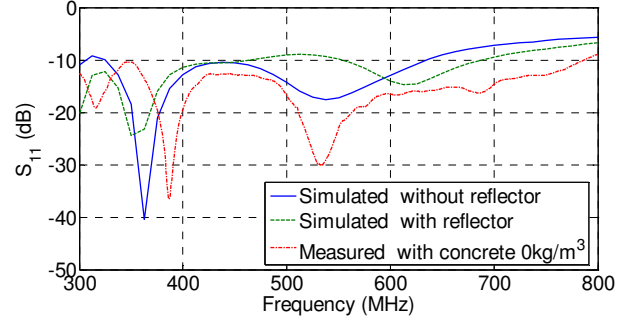


Fig. 6 Simulated and measured return loss of the proposed antenna.

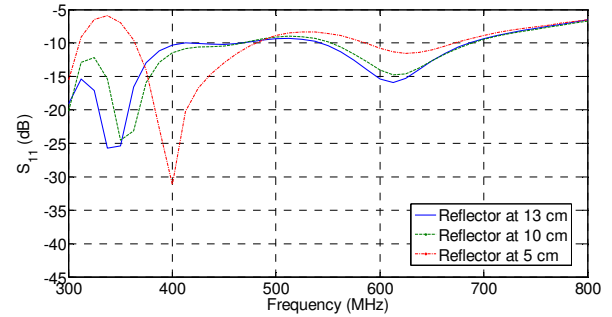


Fig. 7 Simulated return losses for different reflector distances.

Radiation characteristics of the antenna in the total frequency band have also been studied. Fig. 8 shows a non-conventional way to measure the near field radiation pattern of this kind of antenna, which requires the material under test to be considered as well. Two identical antennas are placed on both sides of a standard concrete wall, and linear near-field radiation pattern is captured. Then, distance and phase compensation is applied to transform the linear radiation pattern into a conventional circular radiation pattern, although in near field area. Fig. 9 shows the E and H plane of the measured near field radiation pattern.

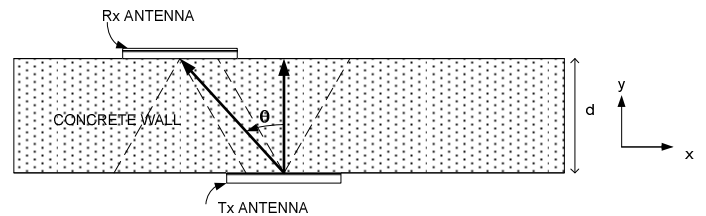


Fig. 8 Radiation pattern measurements setup.

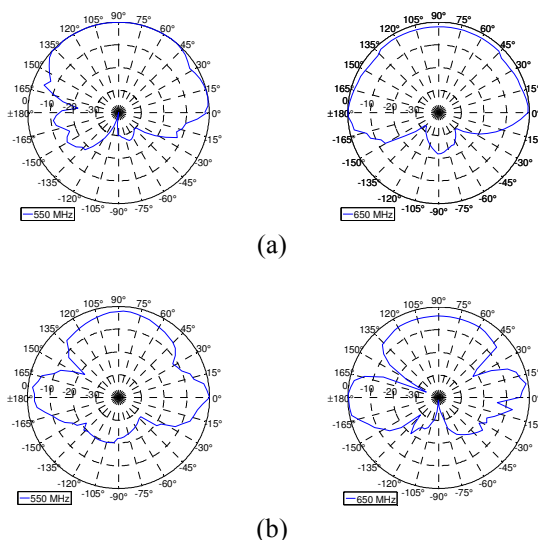


Fig. 9 (a) H plane and (b) E plane at 550 MHz and 650 MHz.

A good cancellation of the back radiation is achieved by means of the strip line reflector along a wide range of frequencies. Front to back ratio along the whole frequency band is greater than 10 dB.

## V. MEASUREMENTS ON CONCRETE

In order to test the antenna performance, concrete wall imaging is carried out, and different SFRC blocs are analysed. Measurements are based on a transmission approach. According to [9], the fiber dosage of a concrete sample can be related to the permittivity of that material using the Maxwell-Garnett approach. The permittivity of the material under test is retrieved from the phase of the transmitted signal using [6], and the reference measurement is a blank concrete wall, that is to say, a concrete wall without fibers.

### A. Concrete wall imaging

A flat concrete wall imaging has been performed in order to determine the sensibility of the measurement system. Fig. 10 a, b and c show the imaging results of analysing a simple blank wall, a blank wall with a metallic object and a blank wall with two metallic objects respectively. The scanning steps are performed such that  $\Delta x=8$  cm and  $\Delta y=15$  cm. Original objects are marked under a red square.

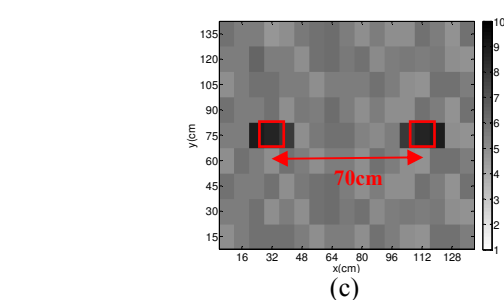
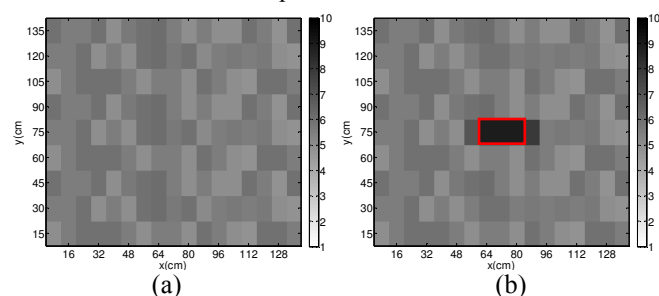


Fig. 10 Permittivity of a (a) blank wall, (b) one metallic object sized  $14 \times 27 \text{ cm}^2$  on the wall and (c) two metallic objects distanced 70 cm and sized  $14 \times 14 \text{ cm}^2$  on the wall.

### B. Concrete slab dielectric characterization

A sequence of labelled concrete slabs has been measured and their permittivity is retrieved following the same procedure than in previous section. The slab sequence belongs to different fiber dosages approaching the standard dosage inside a real concrete dowel used for construction purposes:  $0 \text{ kg/m}^3$ ,  $20 \text{ kg/m}^3$ ,  $40 \text{ kg/m}^3$  and  $60 \text{ kg/m}^3$ . Transmitted phase results and retrieved permittivity are shown in Fig. 11 and Fig. 12 respectively.

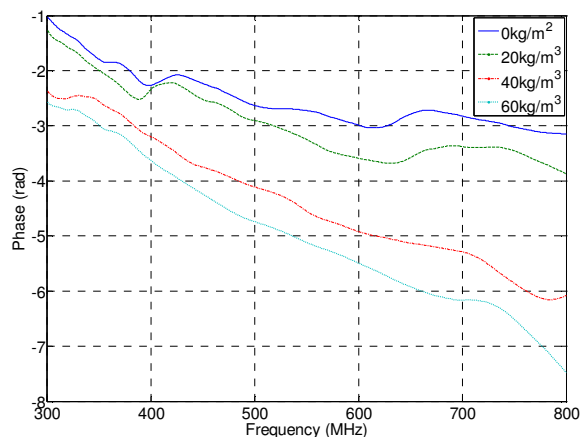


Fig. 11. Phase variation as a function of frequency.

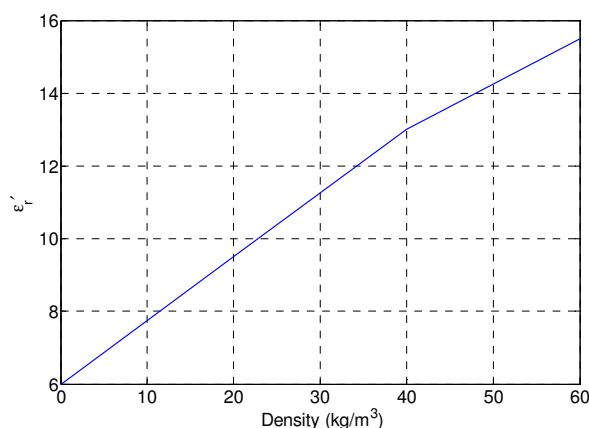


Fig. 12. Permittivity as a function of the fiber density.

## VI. CONCLUSIONS

A compact wideband microstrip slot antenna is designed. This design is matched to concrete medium such that greater penetrability is achieved. Resistive loading has been included to provide a sharp transmitting pulse. Although efficiency is almost reduced to 60%, this is not a major concern in this study, where measurements are taken in near field. The addition of a reflector with optimized dimensions and distance to the ground plane results in a front to back ratio greater than 10 dB, and provides to the antenna immunity from external interferences. This solution provides promising prospects of performing near field measurements of steel fiber reinforced concrete such that radiographic images of its fiber distribution can be obtained. In this context, the antenna performance is experimentally tested and approved. Concrete wall imaging is successfully performed and different labelled SFRC blocs are analysed. A nearly linear relation between the fiber dosage and the permittivity has been obtained, as predicted in the theoretical model based on the Maxwell-Garnet approach [6].

## VII. ACKNOWLEDGMENT

This project arises from the multidisciplinary group joining Signal Theory and Communications department, and Civil Engineering department, headed by Professor Antonio Aguado, to whom special thanks are addressed. Thanks also to Professor J. M. Torrents for his support on the conception of the measurement and procurement of the SFRC samples.

This work was supported in part by the Spanish Interministerial Commission on Science and Technology (CICYT) under projects TEC2007-66698-C04-01/TCM and CONSOLIDER CSD2008-00068 and by the "Ministerio de Educación y Ciencia" through the FPU fellowship program.

## VIII. REFERENCES

- [1] Naaman, A. E. and Reinhardt, H. W. "Fiber reinforced concrete: Current needs for successful implementation". *International Workshop on Advances in Fiber Reinforced Concrete*, Bergamo, Italy.
- [2] Reinhardt, H. W., Grosse, C. U., and Weiler, B. (2001). "Material characterization of steel fiber reinforced concrete using neutron CT, ultrasound and quantitative acoustic emission techniques." *NDT.net*, 6(5).
- [3] Mason, T. O., Campo, M. A., Hixson, A. D., and Woo, L. Y. (2002). "Impedance spectroscopy of fiber reinforced cement composites." *Cement & Concrete Composites*, 24(5), 457-465.
- [4] Peter S. Hall, Y. Hao, "Antennas And Propagation for Body-Centric Wireless Communications", October 2006.
- [5] Y. Yoshimura, "A Reciprocity Method of Analysis for Printed Slot and Slot-Coupled Microstrip Antennas", *IEEE Transactions on Antennas and Propagation*, VOL. AP-34, NO. 12, December 1986.
- [6] G. Roqueta, B. Monsalve, S. Blanch, J. Romeu and L. Jofre, "Microwave Dielectric Properties Inspection of Fiber-Reinforced Civil Structures", *IEEE International Symposium on Antennas and Propagation*, San Diego, July 2008.
- [7] C. A. Balanis, *Antenna Theory: Analysis and Design*, 2nd ed., Wiley, 1997.
- [8] A. S. Abdallah Liu Yuan-an, Y. E. Mohammed, "Wide-Band Wide- Slot Microstrip Antenna", *Radio Science Conference 2004, Proceedings 2004, Asia-Pacific Issue 24-27*, pp. 27-30, August 2004.
- [9] Zhu, L., Fu. R. and Wu K., "A Novel Broadband Microstrip-Fed Wide Slot Antenna With Double Rejection Zeros", *IEEE Antennas and Wireless Propagation Letters*, VOL. 2, pp. 194-196, 2003.
- [10] S. A. Tretyakov, S. Maslovski, P.A. Belov, "An Analytical Model of Metamaterials Based on Loaded Wire Dipoles", *IEEE Trans. on Antennas and propagation*, vol. 51, no. 10, October 2003, pp. 2652-2658